Digital In-line holography: effect of shifted objet in an elliptical, astigmatic gaussian beam

N. Verrier, S. Coëtmellec, M. Brunel and D. Lebrun

Groupe d'Optique et d'Optoélectronique, UMR-6614 CORIA, Av. de l'Université, 76801 Saint-Etienne du Rouvray cedex, France

coetmellec@coria.fr, a.j.e.m.janssen@philips.com

A.J.E.M Janssen

Philips Research Laboratories-Building WO-02, Prof. Holstlaan 4, 5656 AA Eindhoven, The Netherlands

We demonstrate in this paper that the effect of shifted objet in an elliptical, astigmatic gaussian beam does not affect the optimal fractional orders to reconstruct the image of the particle or an other opaque object. Simulations and experimental results are presented.

OCIS codes: 090.0090, 070.0070, 100.0100

1. Introduction

Digital in-line holography (DIH) is widely used in the microscopy for biological applications,[1,2] Particle Image Velocimetry (PIV)[3] and refractometry.[4] In the most DIH theoretical studies, the optical systems or the used objects, for example particles, are considered centered on the optical axis.[5,6] Nevertheless, in many practical applications, the systems are not necessary centered and the objects too. To reconstruct the image of an objet, a reconstruction parameter must be determine. For the wavelet transformation, the parameter is the scale factor.[7] For Fresnel transformation, the

parameter is the distance z between the quadratic sensor and the object[8] and in the case of the fractional Fourier transformation, the parameters are the fractional orders.[9,10] One consider that the same parameter can be used for all positions of the object. Recently, an analytical solution of scalar diffraction of an elliptical and astigmatic Gaussian beam (EAGB) by an centered opaque disk under Fresnel approximation has been proposed. By using the fractional Fourier transformation, a good particle image reconstruction is obtained.[11] Neither can one find recent publications in DIH method developments demonstrated that the parameter of the reconstruction is constant for all positions of the object in the cross-plan.

In this publication, the aim is to demonstrate that the same fractional orders are necessary to reconstruct an image of the particle. We exhibits the effect of the gaussian beam of the reconstructed image. In the first part of this publication, the model of the analytical solution of scalar diffraction of an EAGB by a centered opaque disk is revisited to take into account a decentered object. In the second part, the definition of the fractional Fourier transformation is recalled and this transformation is used to reconstruct the image of the particle. It is in this part that one demonstrate the same orders are is necessary. Finally, we propose to illustrate our results by numerical experiments and experimental result.

2. In-Line Holography with an elliptic and astigmatic Gaussian beam

The idea of the DIH consists to record by the CCD camera the intensity distribution of the diffraction pattern of an objet illuminated by a continue or not wave. The basic model to describe the intensity distribution recorded by the CCD camera of an objet is the integral of Kirchhoff-Fresnel given by the scalar integral:

$$A = \frac{\exp(i\frac{2\pi}{\lambda}z)}{i\lambda z}\int_{\mathbb{R}^2} E_T(\xi,\eta)\,\exp\left(\frac{i\pi}{\lambda z}\left[(\xi-x)^2+(\eta-y)^2\right]\right)d\xi d\eta, \tag{1}$$

in which $E_T(\xi,\eta)$ is the product of the optical incident beam, noted here by $E(\xi,\eta)$, by the spatial transmittance of the shifted opaque 2D-object, noted $1-T(\xi-\xi_0,\eta-\eta_0)$, and A is the complex

amplitude in the quadratic sensor plane. The quadratic sensor records the intensity defined by $|A|^2$. If we consider that the function E_T is the product of an elliptic and astigmatic Gaussian beam by an opaque disk of diameter D, then

$$E_T(\xi,\eta) = \underbrace{\exp\left[c_\xi \xi^2 + c_\eta \eta^2\right]}_{=E(\xi,\eta)} \cdot \underbrace{\left[1 - T(\xi-\xi_0, \eta-\eta_0)\right]}_{shifted\ object}. \tag{2}$$

The complex coefficients c_ξ and c_η are

$$c_\xi = -\frac{1}{\omega_\xi^2} - i\frac{\pi}{\lambda R_\xi}, \quad c_\eta = -\frac{1}{\omega_\eta^2} - i\frac{\pi}{\lambda R_\eta} \tag{3}$$

R_q with $q = \xi, \eta$ are the wavefront curvatures and ω_q denote the beam widths along the ξ-axis and η-axis. These four parameters are defined in the object plane. For an opaque disk centered at the origin O, the transmittance function $T(\xi,\eta)$ in the object plane is:

$$T(\xi,\eta) = \begin{cases} 1, & 0 < \sqrt{\xi^2+\eta^2} < D/2, \\ 1/2, & 0 < \sqrt{\xi^2+\eta^2} = D/2, \\ 0, & \sqrt{\xi^2+\eta^2} > D/2 > 0. \end{cases} \tag{4}$$

From Eqs (1) and (2), the expression of $A(x,y)$ can be can splited in two integral terms, noted A_1 and A_2, such as:

$$A(x,y) = \frac{\exp(i\frac{2\pi}{\lambda}z)}{i}\left[A_1 - A_2\right]. \tag{5}$$

2.A. Expression for the amplitude distribution A_1

The development of integral A_1, versus $E(\xi,\eta)$, is given in a previous paper by[11] :

$$A_1 = K_\xi K_\eta \exp\left(-\frac{\pi}{\lambda z}\rho^{\mathrm{T}} N \rho\right) \exp\left(i\frac{\pi}{\lambda z}\rho^{\mathrm{T}} M \rho\right) \tag{6}$$

where ρ^{T} represents the vector $(x \quad y)$ and the factors K_q with $q = \xi, \eta$ in Eq.(6) are defined by

$$K_q = \left[\frac{\frac{\pi\omega_q^2}{\lambda z}}{1 + i\frac{\pi\omega_q^2}{\lambda z}\left(\frac{z}{R_q} - 1\right)}\right]^{1/2} \tag{7}$$

and the diagonal matrices N and M by

$$N = \begin{pmatrix} N_x & 0 \\ 0 & N_y \end{pmatrix}, \qquad M = \begin{pmatrix} M_x & 0 \\ 0 & M_y \end{pmatrix}, \tag{8}$$

with

$$N_q = \pi \frac{\frac{\omega_q^2}{\lambda z}}{1 + \pi^2 \frac{\omega_q^4}{(\lambda z)^2} \left(\frac{z}{R_q} - 1\right)^2} \quad , \quad M_q = 1 + \pi^2 \frac{\frac{\omega_q^4}{(\lambda z)^2} \left(\frac{z}{R_q} - 1\right)}{1 + \pi^2 \frac{\omega_q^4}{(\lambda z)^2} \left(\frac{z}{R_q} - 1\right)^2}. \tag{9}$$

2.B. Expression for the amplitude distribution A_2

To develop the second integral of A_2, only versus the product between $E(\xi, \eta)$ by $T(\xi - \xi_0, \eta - \eta_0)$, *i.e.*:

$$A_2 = \frac{\exp\left[\frac{i\pi}{\lambda z}(x^2 + y^2)\right]}{\lambda z} \int_{\mathbb{R}^2} E(\xi, \eta) T(\xi - \xi_0, \eta - \eta_0) \exp\left[\frac{i\pi}{\lambda z}(\xi^2 + \eta^2)\right] \exp\left[-i\frac{2\pi}{\lambda z}(x\xi + y\eta)\right] d\xi d\eta, \tag{10}$$

firstly ξ is replaced by $\xi + \xi_0$ and η by $\eta + \eta_0$, then we have:

$$A_2 = \frac{\exp\left[\frac{i\pi}{\lambda z}(x^2 + y^2)\right]}{\lambda z} \int_{\mathcal{D}} E(\xi + \xi_0, \eta + \eta_0) \exp\left[\frac{i\pi}{\lambda z}((\xi + \xi_0)^2 + (\eta + \eta_0)^2)\right] \times \exp\left[-i\frac{2\pi}{\lambda z}(x(\xi + \xi_0) + y(\eta + \eta_0))\right] d\xi d\eta. \tag{11}$$

By considering that $c_z = \pi/(\lambda z)$ and by restating A_2 in cylindrical coordinates as follows: $\xi = D\sigma\cos(\varphi)/2$ and $\eta = D\sigma\sin(\varphi)/2$ for the object plane, we obtain:

$$A_2 = \frac{D^2}{4\lambda z} \exp\left[c_\xi \xi_0^2 + c_\eta \eta_0^2 + i c_z \left[(x - \xi_0)^2 + (y - \eta_0)^2\right]\right] \cdot \int_0^1 \int_0^{2\pi} \exp\left[i\gamma\sigma^2\right] \exp\left[i\delta\sigma^2\cos(2\varphi)\right] \exp\left[ia\sigma\cos\varphi + ib\sigma\sin\varphi\right] \sigma d\sigma d\varphi \tag{12}$$

with

$$\gamma = \frac{D^2}{4} c_z - i\frac{D^2}{8}(c_\xi + c_\eta), \qquad \delta = i\frac{D^2}{8}(c_\eta - c_\xi),$$
$$a = Dc_z\left[\xi_0(1 - ic_\xi/c_z) - x\right], \qquad b = Dc_z\left[\eta_0(1 - ic_\eta/c_z) - y\right]. \tag{13}$$

By writing that:

$$a\cos\varphi + b\sin\varphi = r\cos(\varphi - \theta) \tag{14}$$

for which we have the condition

$$a = r\cos\theta, \qquad b = r\sin\theta \tag{15}$$

with complex r and θ. This representation is discussed in some detail in Appendix A. By means of the following equalities in [12], 4.9.3 - 4.9.6 on p. 210-211:

$$\exp\left[i\delta\sigma^2\cos\left(2\varphi+2\theta\right)\right] = J_0\left(\delta\sigma^2\right) + 2\sum_{k=1}^{+\infty} i^k J_k\left(\delta\sigma^2\right)\cos 2k(\varphi+\theta), \tag{16}$$

and

$$\frac{1}{2\pi}\int_0^{2\pi}\exp(in\theta)\exp[ix\cos\theta]d\theta = i^n J_n(x), \tag{17}$$

The expression of A_2 becomes:

$$A_2 = \frac{\pi D^2}{\lambda z}\exp\left[\Phi(\xi_0,\eta_0)\right]\cdot\exp\left(ic_z\left[(x-\xi_0)^2+(y-\eta_0)^2\right]\right)\cdot\sum_{k=0}^{\infty}(-i)^k\varepsilon_k\, T_k(r,\gamma)\cos(2k\theta), \tag{18}$$

with $\varepsilon_k = 1/2$ if $k = 0$ and 1 otherwise. The parameter noted $\Phi(\xi_0,\eta_0)$ is equal to $\left[c_\xi\xi_0^2 + c_\eta\eta_0^2\right]$. The function $T_k(r,2\gamma)$ is defined as:

$$T_k(r,\gamma) = \sum_{p=0}^{\infty}\beta_{2k+2p}^{2k}(\delta)V_{2k+2p}^{2k}(r,\gamma), \tag{19}$$

where the coefficients β_{2k+2p}^{2k} are given by the analytical development of T_k in Appendix of [11]. Recall here that the expression of $V_{2k+2p}^{2k}(r,\gamma)$ is:

$$V_{2k+2p}^{2k}(r,\gamma) = \exp(i\gamma/2)\sum_{m=0}^{\infty}(2m+1)i^m j_m(\gamma/2)\cdot\sum_{l=\max(0,m-2k-p,p-m)}^{m+p}(-1)^l\omega_{ml}\frac{J_{2k+2l+1}(r)}{r}. \tag{20}$$

Finally, the expression of A_1 contents only the characteristics of the incident beam and A_2 contents a shifted linear chirp function linked to the decentered of the object. The previous function is modulated by a summation of bessel function which constitutes the envelop of the amplitude distribution of A_2.

Now, to obtain the desired accuracy, we would analyse the number of terms necessary in the series over k in (18) and over p in (19). The series which would be analyse are in the Eq.(20). The first upper bound that one can be considered is[13–15]

$$\left|j_m\left(\frac{\gamma}{2}\right)\right| \le \frac{1}{(2m+1)^{1/2}}\,\min\left(1,\left(\frac{\pi}{2}\right)^{1/2}\frac{|\gamma/4|^m}{m!}\right). \tag{21}$$

The evaluation of the function $\left|j_m\left(\frac{\gamma}{2}\right)\right|$ is versus the rough estimate of the variable γ. As $D \approx 10^{-4}m$, $\lambda \approx 10^{-6}m$, $z \approx 10^{-1}m$, $R_q \approx 0.5 \cdot 10^{-1}$ then $\gamma \approx 0.785 \cdot 10^{-1} + 0.816 \cdot 10^{-3}i$. All the quantities in (21) are less than $0.142 \cdot 10^{-1}$ for $m \geq 1$. The second upper bound is link to the Bessel function such as from [16], 9.1.62 on p.362 and [13], one have

$$\left|\frac{J_{2k+2l+1}(r)}{r}\right| \leq \min\left(1, \frac{1}{2}\frac{|r|^{2k+2l}\exp(|r|^2)}{(2k+2l+1)!}\right) \tag{22}$$

The evaluation of the accuracy is versus the following product of the Eqs. (21) and (22):

$$\left|j_m\left(\frac{\gamma}{2}\right)\right| \left|\frac{J_{2k+2(m+p)+1}(r)}{r}\right| \tag{23}$$

With the previous values, all the quantities in (23) are less than $0.142 \cdot 10^{-1}$ for all $(k, p, m) \geq 1$. Finally, we only consider the case where $k = p = m = 0$. The function $V_{2k+2p}^{2k}(r, \gamma)$ which will be used with a good accuracy in our case is defined by:

$$V_0^0(r, \gamma) \simeq \exp(i\gamma/2) j_0(\gamma/2) \frac{J_1(r)}{r}. \tag{24}$$

The amplitude A_2 becomes then

$$A_2 = \frac{\pi D^2}{2\lambda z}\beta_0^0(\delta)\exp\left[\Phi(\xi_0, \eta_0)\right]\exp\left(ic_z\left[(x-\xi_0)^2 + (y-\eta_0)^2\right]\right) \cdot V_0^0(r, \gamma), \tag{25}$$

2.C. Intensity distribution of the diffraction pattern

The intensity distribution of the diffraction pattern in the quadratic sensor plane, noted I, is evaluated from the Eqs. (5) (6) and (25) in the following way:

$$I = A\overline{A} = [A_1 - A_2]\left[\overline{A_1} - \overline{A_2}\right] = \left[|A_1|^2 + |A_2|^2\right] - 2\,\Re\left\{A_1\overline{A_2}\right\} \tag{26}$$

where the over line denotes the complex conjugate, $\Re$ denotes the real part. Thus, the intensity distribution recorded by the CCD sensor is described by the Eq. (26). As one can see from the relation of I is that the first and second terms, i.e. $|A_1|^2$ and $|A_2|^2$, not generate interference fringes with a linear chirp in the plane of the CCD. But the third term exhibits a phase which composed of a constant and linear instantaneous frequencies. This fact is important because the fractional Fourier

transform is an efficiency operator to analyse the linear instantaneous frequency. From Eq. (26) we write

$$A_1\overline{A_2} = |A_1\overline{A_2}| \exp\left[i \arg\left(A_1\overline{A_2}\right)\right] \tag{27}$$

where $\arg\left(A_1\overline{A_2}\right) = \phi - \phi_0$ with

$$\phi = c_z\left(x^2(M_\xi - 1) + y^2(M_\eta - 1)\right) + 2c_z\left(x\xi_0 + y\eta_0\right) - \arg\left(\frac{J_1(r)}{r}\right), \tag{28}$$

and

$$\phi_0 = \frac{\Re(\gamma)}{2} + \Im(\Phi(\xi_0, \eta_0)) + \arg\left(j_0\left(\frac{\gamma}{2}\right)\right) + \arg\left(\beta_0^0(\delta)\right) - \arg\left(K_\xi K_\eta\right), \tag{29}$$

where $\Re$ and $\Im$ represent the real and imaginary parts of a complex number. The first term in (28) is versus a quadratic phase and the second is a linear phase. Recall that the aim of the reconstruction by means of the FRFT is precisely to analyze a linear chirp and only the terms versus of x and y.

To give two different examples, it is necessary to fix the values of the parameters $(\omega_\xi, \omega_\eta)$, (R_ξ, R_η) and (D, λ, z). The figure (1) represents the numerical and experimental set-up where all parameters are identified. The first four parameters are defined in the plane of the object. To do this, it is necessary to specify the values of (Δ, δ) which are the algebraic distance between the cylinder lens (CL) and the particle and the distance between the beam waist and the particle.

In the first case, the values are defined by $(7mm, 1.75mm)$ for the beam waists, $(-\infty, -50mm)$ for the wave's curvatures and the diameter D of the particle is equal to $150\mu m$ and located at $120mm$ of the CCD sensor. The wavelength of the laser beam is $632.8nm$. The distance between the cylinder lens and the particle is $\delta = 250mm$. The shifted-particle from the origin is $(\xi_0, \eta_0) = (0.5mm, 0.2mm)$. The figure (2) illustrates the diffraction pattern which recorded by the camera. Note that the shift (x_0, y_0) in the plane of the camera don't equal to the shift (ξ_0, η_0). If the particle is considered far from the waist then we have the formula:

$$y_0 = \frac{\mid \Delta \mid \pm z}{\mid \Delta \mid}\ \eta_0 \tag{30}$$

The sign of z depends of the position of the particle compared to the position of the waist. If the particle is next the waist, the sign is positive. If it is before the waist, the sign is negative. In the case of x-axis, the parameter Δ is infinite so that in the plane of the camera $x_0 = \xi_0 = 0.5mm$ and in the case of y-axis, $\Delta = 50mm$ thus $y_0 = 0.68mm$.

Now, In the second case, the values are defined by $(7mm, 1.75mm)$ for the beam waists, $(-\infty, 50mm)$ for the wave's curvatures and the diameter D of the particle is equal to $150\mu m$ and located at $120mm$ of the CCD sensor. The wavelength of the laser beam is $632.8nm$. The distance between the cylinder lens and the particle is $\delta = 150mm$. The shifted-particle from the origin is $(\xi_0, \eta_0) = (0.5mm, 0.2mm)$. The figure (3) illustrates the diffraction pattern which recorded by the camera. In the plane of the camera, from the equation (30), $x_0 = \xi_0 = 0.5mm$ and in the case of y-axis, $\Delta = 50mm$ thus $y_0 = -0.28mm$. The diffraction pattern changes from elliptical fringes to hyperbolical fringes. These diffraction patterns will be used to reconstruct the image of the particle by the FRFT.

3. Fractional Fourier transformation analysis of in-line holograms

3.A. Two-dimensional Fractional Fourier transformation

The FRFT is an integral operator where it find a lot of application in signal processing, image processing. Its principal advantage is to transform a linear chirp into a Dirac impulse. Its mathematical definition is as follows:[17–19] the two-dimensional fractional Fourier transformation of order a_x for x-cross-section and a_y for y-cross-section with $0 \leq |\alpha_x| \leq \pi/2$ and $0 \leq |\alpha_y| \leq \pi/2$, respectively, of a 2D-function $I(x, y)$ is defined as (with $\alpha_p = \frac{a_p \pi}{2}$)

$$\mathscr{F}_{\alpha_x,\alpha_y}[I(x,y)](x_a, y_a) = \int_{\mathbb{R}^2} N_{\alpha_x}(x, x_a)\, N_{\alpha_y}(y, y_a) I(x, y)\, dx\, dy \tag{31}$$

where the kernel of the fractional operator is defined by

$$N_{\alpha_p}(x, x_a) = C(\alpha_p) \exp\left(i\pi \frac{x^2 + x_a^2}{s_p^2 \tan\alpha_p}\right) \exp\left(-\frac{i2\pi x_a x}{s_p^2 \sin\alpha_p}\right), \tag{32}$$

and

$$C(\alpha_p) = \frac{\exp(-i(\frac{\pi}{4}\text{sign}(\sin\alpha_p) - \frac{\alpha_p}{2}))}{|s_p^2 \sin\alpha_p|^{1/2}}\,. \tag{33}$$

Here $p = x, y$. Generally, the parameter s_p is considered as a normalization coefficient. It can take any values. This incertitude is not acceptable in our case. So, its value is defined from the experimental set-up such as

$$s_p^2 = N_p \cdot \delta_p^2 \tag{34}$$

This definition is presented in Appendix B. N_p is the dimension of the image $I(x, y)$ along x and y-cross axis. The constant δ_q is the sampling period along the two previous axis of the image. In our case the size of the image and the sampling period are the same along the two axis. So that the parameters s_p are equal to s. The energy-conservation law is ensured by the coefficient $C(\alpha_p)$ which is a function of the fractional order.

3.B. Reconstruction: optimal fractional orders

To reconstruct the image of the particle, the following transform must be calculated:

$$\mathscr{F}_{\alpha_x,\alpha_y}[I] = \mathscr{F}_{\alpha_x,\alpha_y}\left[|A_1|^2\right] - \mathscr{F}_{\alpha_x,\alpha_y}\left[2|A_1\overline{A_2}|\cos(\phi - \phi_0)\right] + \mathscr{F}_{\alpha_x,\alpha_y}\left[|A_2|^2\right] \tag{35}$$

The terms $|A_1|^2$ and $|A_2|^2$ are not versus linear chirp thus they do not have an effect on the optimal fractional order to determine. But the second term, noted S_t is expressed versus the linear chirp. It will be considered for the image reconstruction of the particle. By noting that $2\cos(\phi - \phi_0) = \exp(-i(\phi - \phi_0)) + \exp(i(\phi - \phi_0))$, the second term of Eq. (35) becomes :

$$\mathscr{F}_{\alpha_x,\alpha_y}\left[2|A_1\overline{A_2}|\cos(\phi - \phi_0)\right] = \exp\left(i\pi\frac{x_a^2}{s^2\tan\alpha_x}\right)\exp\left(i\pi\frac{y_a^2}{s^2\tan\alpha_y}\right)\{I_- + I_+\} \tag{36}$$

with

$$I_\pm = C(\alpha_x)C(\alpha_y)\iint_{\mathbb{R}^2}\left|A_1\overline{A_2}\right|\exp\left[i\left(\phi_a \pm (\phi - \phi_0)\right)\right]\exp\left[-\frac{2i\pi}{s^2}\left(\frac{x_a x}{\sin\alpha_x} + \frac{y_a y}{\sin\alpha_y}\right)\right]dxdy \tag{37}$$

The quadratic phase term of the FRFT is noted by $\phi_a = \frac{\pi}{s^2}\left(x^2\cot\alpha_x + y^2\cot\alpha_y\right)$. Let us recall that the FRFT allow us to analyze a linear chirp. For I_-, if

$$\frac{\pi\cot\alpha_x^{opt}}{s^2} = c_z(M_x - 1), \qquad \frac{\pi\cot\alpha_y^{opt}}{s^2} = c_z(M_y - 1), \tag{38}$$

then, the FRFT is only a classical Fourier transformation such as

$$I_- = \chi\cdot\mathcal{F}\left[\frac{J_1(r)}{r}\cdot\exp\left(-\frac{\pi}{\lambda z}\rho^{\mathrm{T}}N\rho\right)\right](u,v), \tag{39}$$

with $\chi = \frac{\pi D^2}{2\lambda z}C(\alpha_x)C(\alpha_y)K_\xi K_\eta\exp\left[\Phi(\xi_0,\eta_0)\right]\beta_0^0(\delta)\exp\left(i\frac{\gamma}{2}\right)j_0\left(\frac{\gamma}{2}\right)$. The operator $\mathcal{F}$ is the 2D-Fourier transformation. The spatial frequencies u and v are equal to:

$$u = \frac{x_a}{s^2\sin(\alpha_x^{opt})} + \frac{c_z\xi_0}{\pi} \qquad v = \frac{y_a}{s^2\sin(\alpha_y^{opt})} + \frac{c_z\eta_0}{\pi} \tag{40}$$

As Fourier transform of the multiplication of two functions means convolution of their transforms then

$$I_- = \chi\cdot\mathcal{F}\left[\frac{J_1(r)}{r}\right] * \mathcal{F}\left[\exp\left(-\frac{\pi}{\lambda z}\rho^{\mathrm{T}}N\rho\right)\right], \tag{41}$$

Recall here that the variables ρ and r are versus the same coordinates (x,y). With the shift theorem for the Fourier transform, the Hankel transform and the discontinuous Weber-Schafheitlin integral on [16], 11.4.42 on p.487, we have:

$$\mathcal{F}\left[\frac{J_1(r)}{r}\right] = 2\pi\left(\frac{\lambda z}{\pi D}\right)^2\exp\left[-i2\pi(uX_0+vY_0)\right]\times\begin{cases}1, & 0<\sqrt{u^2+v^2}<\frac{D/2}{\lambda z},\\ 1/2, & 0<\sqrt{u^2+v^2}=\frac{D/2}{\lambda z},\\ 0, & \sqrt{u^2+v^2}>\frac{D/2}{\lambda z}>0,\end{cases} \tag{42}$$

with $X_0 = \xi_0\left(1 - ic_\xi/c_z\right)$ and $Y_0 = \eta_0\left(1 - ic_\eta/c_z\right)$. The function defined by the right term of (42), versus the spatial coordinates (x_a, y_a), has the aperture of the pinhole equal to the diameter D of the opaque particle. The shifting of the object does not modify the fractional order. This point is important because in the case of particle field one fractional order along x-cross axis and y-cross axis is necessary to reconstruct the image of the particles. If one want to determine the position of

the center of the diffraction patterns in the plan (x_a, y_a), the coordinates that could be considered must be:

$$\left(s^2(u - \frac{c_z\xi_0}{\pi})\tan\alpha_x^{opt}, s^2(v - \frac{c_z\eta_0}{\pi})\tan\alpha_x^{opt}\right) \tag{43}$$

This correction is necessary because the fractional Fourier transformation is non linear by translation. Note that the nature of the gaussian beam implies that the reconstructed image of the object is convoluted by Gaussian. The opaqueness of the object is retrieved by applying an inversion of I_- that is realized by the minus in front of the second term of the equation (35). The dynamic of the amplitude of the signal as in the Eq. (4) is ensured by the gaussian function defined by the first term of (35).

3.C. Numerical experiments

The simulations of the reconstruction of the image of a particle are realized from the diffraction patterns illustrated by the Figs. (2) and (3). The diffraction patterns consist of 512×512 array of $11\mu m \times 11\mu m$ size pixels. Consider the diffraction pattern presented in Fig. (2) of diameter $D = 150\mu m$ particle located at $z = 120mm$. The optimal fractional orders obtained from Eqs. (38) are $a_x^{opt} = -0.564$ and $a_y^{opt} = -0.850$. The image of the reconstructed image is shown in Fig. (4). In this representation, the squared modulus of the FRFT, *i.e.* $|\mathscr{F}_{\alpha_x,\alpha_y}[I]|^2$, is taken. The shape of the image of the particle is not modify: the width of the gaussian function in the Eq.(41) is greater than the diameter D of the particle (typically $679\mu m$ along x-cross axis and $490\mu m$ along y-cross axis). Now, the reconstruction of the image of the particle from the diffraction pattern illustrated by the Fig. (3), is realized by a fractional Fourier transformation of optimal orders $a_x^{opt} = -0.564$ and $a_y^{opt} = 0.664$. The Fig. (5) illustrates the result of the reconstruction. Note that the apertures of the result of the Eq. (41) and the image of the reconstructed particle have been verified and give the same diameter D.

3.D. Experimental result

The previous theoretical developments and numerical experiments have been tested by using an RS-3 standard reticle (Malvern Equipment). This reticle is an optical glass plate with a pattern of the word LASER photographically deposited on the surface. This reticle is localized at $\delta = 249mm$ from the cylindrical lens (CL). The distance z between the CCD camera and the reticle is equal to $117mm$. The opaque word "LASER" is next the waist of the beam. The intensity distribution of the EAGB diffracted by the the word "LASER" is shown in Fig. (6). The reconstruction of the image of the word "LASER" is realized by the fractional Fourier transformation of approximatively orders $a_x^{opt} = 0.559$ and $a_y^{opt} = 0.848$. The two previous orders allows to reconstruct all parts of the image of the object.

4. Conclusion

The effect of shifted objet in an elliptical, astigmatic gaussian beam does not affect the optimal fractional orders to reconstruct the image of the particle or an other opaque object. In this publication an analytical model has been developed to prove that. In this development, the object is an opaque particle and in the experimental result, the particle is replaced by the word "LASER". The advantage of the "LASER" word is that it is spread out over all the image's field.

A. Appendix A : Elaboration of condition (15)

With $u = a + ib$, $v = a - ib$, we should find τ and $\omega = \exp(i\theta)$ such that

$$\tau\omega = u, \qquad \tau/\omega = v \tag{44}$$

Assume that $u \neq 0$, $v \neq 0$, and write $u = r\exp(i\alpha)$, $v = s\exp(i\beta)$ with $r, s > 0$ and $\alpha, \beta \in \mathbb{R}$ then we see that $\omega = \exp(i\theta)$ such that

$$\tau = (rs)^{1/2}\exp\left(i(\alpha+\beta)/2\right), \qquad \omega = \exp(i\theta) = \left(\frac{r}{s}\right)^{1/2}\exp\left(i(\alpha-\beta)/2\right) \tag{45}$$

satisfy the relations (44). This does not work in the case that $u = 0$ or $v = 0$. Indeed, when $a = 1$, $b = i$ we get from (15) and $\cos^2\theta + \sin^2\theta = 1$ that $r = a + ib = 0$, *i.e.* $r = 0$.

B. Appendix B : Definition of s_p

To determine the value of s_p, it is necessary to write the definition of the one dimensional fractional Fourier transformation in the particular case of $\alpha = \pi/2$:

$$\mathcal{F}_{\pi/2}[I(x)](x_a) = C(\pi/2)\int_{-\infty}^{+\infty} I(x)\exp\left(-i2\pi\frac{xx_a}{s^2}\right)dx. \tag{46}$$

Its discrete version is

$$\mathcal{F}_{\pi/2}[I(m)](k) = C(\pi/2)\sum_{m=-N/2}^{N/2-1} I(m)\exp\left(-i2\pi\frac{m\delta_x\ k\delta_{x_a}}{s^2}\right)\delta_x, \tag{47}$$

where δ_x and δ_{x_a} are the sampling periods of $I(x)$ and its transform. The sampling periods are equal to δ_x. N is the number of sampling of $I(x)$ and its transform. The relation (47) can be written as the discrete Fourier transformation of $I(m)$ such as:

$$\mathcal{F}_{\pi/2}[I(m)](k) = C(\pi/2)\sum_{m=-N/2}^{N/2-1} I(m)\exp\left(-i2\pi\frac{mk}{N}\right)\delta_x. \tag{48}$$

By identification of Eqs. (48) and (47), one obtain:

$$\frac{\delta_x\delta_{x_a}}{s^2} = \frac{1}{N} \Rightarrow s^2 = N\delta_x\delta_{x_a} = N\delta_x^2 \tag{49}$$

In the case of bidimensional function one finally have $s_p^2 = N_p \cdot \delta_p^2$ with $p = \xi, \eta$

Acknowledgments

The authors thank F. Nicolas for passing images (6) and (7) to them.

References

1. W. Xu, M. H. Jericho, H. J. Kreuzer, and I. A. Meinertzhagen, "Tracking particles in four dimensions with in-line holographic microscopy", Opt. Lett. 28, 164-166 (2003).
2. F. Dubois, L. Joannes, and J.-C. Legros, "Improved three-dimensional imaging with digital holography microscope using a partial spatial coherent source," Appl. Opt. 38, 7085-7094 (1999).
3. B. Skarman, K. Wozniac, and J. Becker, "Simultaneous 3D-PIV and temperature measurement using a new CCD based holographic interferometer," Flow Meas. Instrum. 7, 1-6 (1996).
4. M. Sebesta and M. Gustafsson, "Object characterization with refractometric digital Fourier holography," Opt. Lett. 30, 471-473 (2005).
5. U. Schnars, "Direct phase determination in hologram interferometry with use of digitally recorded holograms," J. Opt. Soc. Am. A 11, 2011- (1994).
6. Gongxin Shen and Runjie Wei, "Digital holography particle image velocimetry for the measurement of 3Dt-3c flows," Optics and Lasers in Engineering **43**, 1039-1055 (2002).
7. L. Onural, "Diffraction from a wavelet point of view," Opt. Lett. 18, 846-848 (1993)
8. L. Onural P. D. Scott, "Digital decoding of in-line holograms," Opt. Engineering 26, 1124-1132 (1987)
9. Eric Fogret and Pierre Pellat-Finet, "Agreement of fractional Fourier optics with the Huygens Fresnel principle", Optics Communications 272, 281-288 (2007)
10. S. Coëtmellec, D. Lebrun, and C. Özkul, "Characterization of diffraction patterns directly from in-line holograms with the fractional Fourier transform," Appl. Opt. 41, 312-319 (2002)
11. F. Nicolas, S. Coëtmellec, M. Brunel, D. Allano, D. Lebrun, and A. J. Janssen, "Application of the fractional Fourier transformation to digital holography recorded by an elliptical, astigmatic Gaussian beam," J. Opt. Soc. Am. A 22, 2569-2577 (2005).
12. G. E. Andrews, R. Askey, and R. Roy, Special Functions, *Cambridge University Press*, Cam-

bridge, 210-211 (1999).

13. A.J.E.M. Janssen, J.J.M. Braat and P. Dirksen, "On the computation of the Nijboer-Zernike aberration integrals at arbitrary defocus ", J. Mod. Optics, **51**, n°5, 687–703 (2004).

14. J.J.M. Braat, P. Dirksen and A.J.E.M. Janssen, "Assessment of an extended Nijboer-Zernike approach for the computation of optical point-spread functions", J. Opt. Soc. Am. A **19**, 858–870 (2002).

15. A.J.E.M. Janssen, "Extended Nijboer-Zernike approach for the computation of optical point-spread functions", J. Opt. Soc. Am. A **19**, 849-857 (2002).

16. Abramowitz and Stegun, Handbook of Mathematical Functions, *Dover Publications, Inc., New York*, (1970).

17. A.C. McBride and F.H. Kerr, "On Namias's Fractional Fourier Transforms", IMA J. Appl. Math. **39**, 159–175 (1987).

18. V. Namias, "The fractional Order Fourier Transform and its Application to quantum Mechanics", J. Inst. Maths Its Applics, **25**, 241–265 (1980).

19. A. W. Lohmann , "Image rotation, Wigner rotation, and the fractional Fourier transform", J. Opt. Soc. Am. A **10**, 2181–2186 (1993).

List of Figures

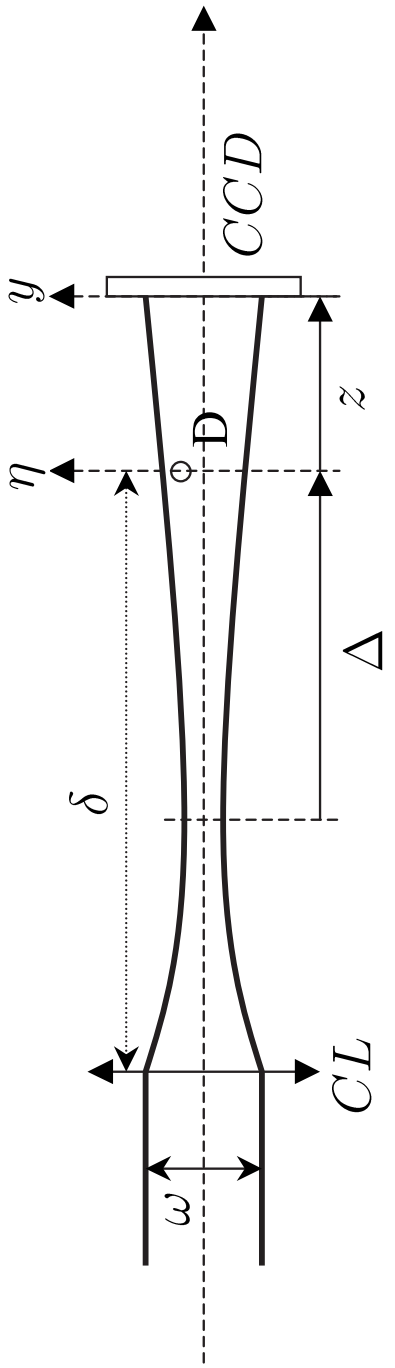

Fig. 1. Numerical and Experimental optical set-up.

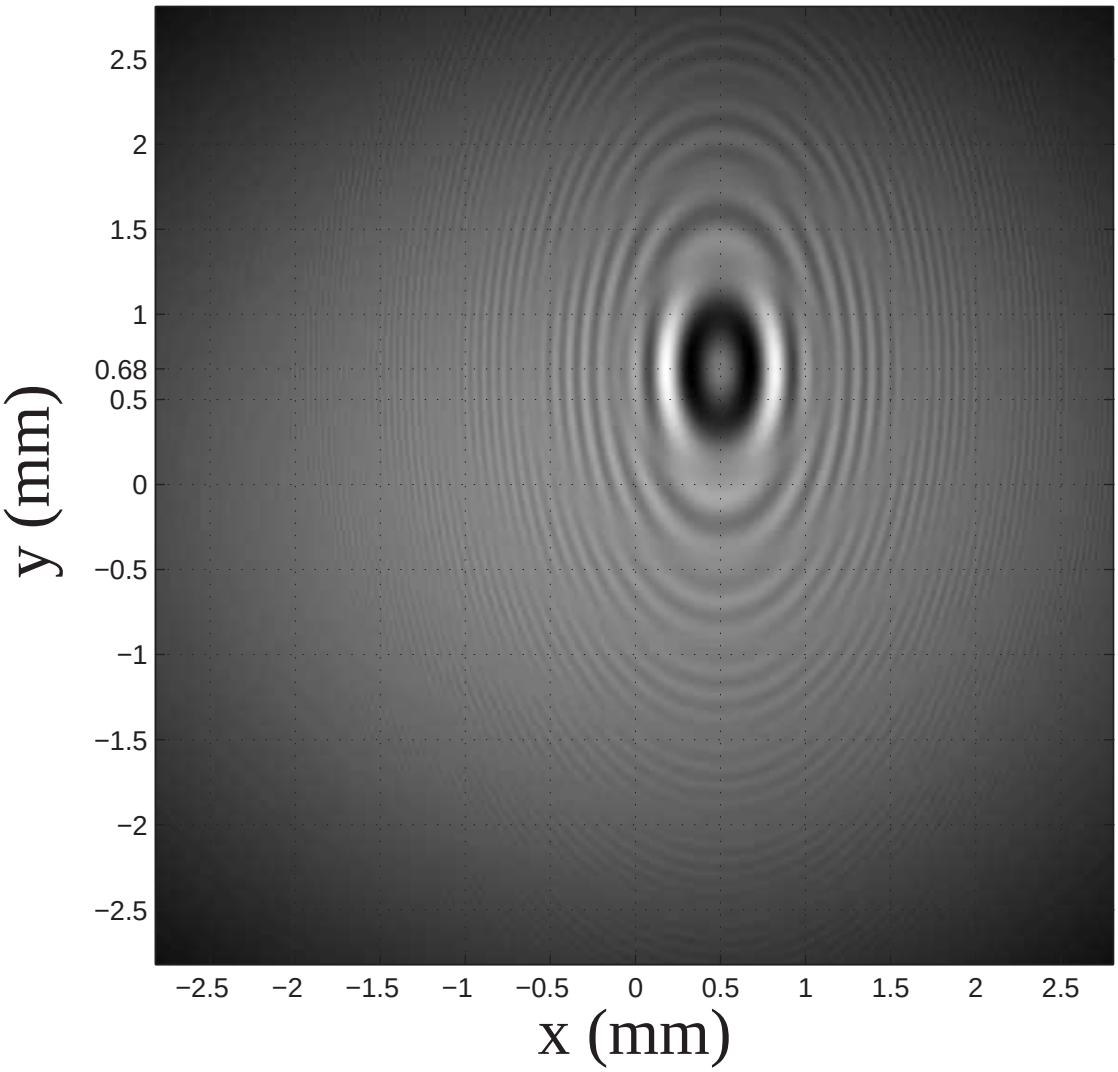

Fig. 2. Diffraction pattern with , $\omega_\xi = 7mm$, $\omega_\eta = 1.75mm$, $R_\xi = \infty$, $R_\eta = -50mm$, $D = 150\mu m$, $\lambda = 632.8nm$, $z = 120mm$, $\delta = 250mm$, $\xi_0 = 0.5mm$ and $\eta_0 = 0.2mm$

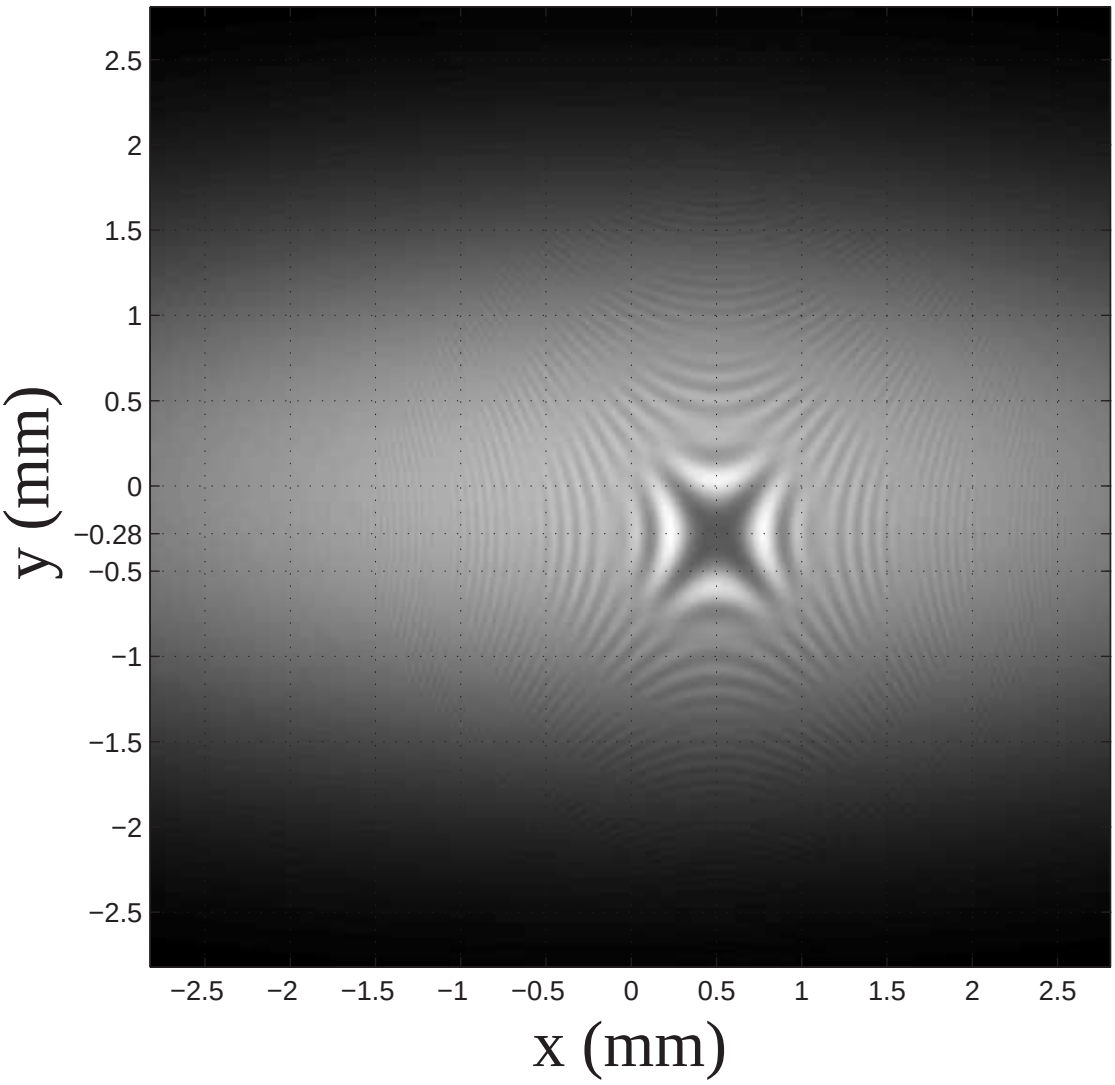

Fig. 3. Diffraction pattern with , $\omega_\xi = 7mm$, $\omega_\eta = 1.75mm$, $R_\xi = \infty$, $R_\eta = -50mm$, $D = 150\mu m$, $\lambda = 632.8nm$, $z = 120mm$, $\delta = 150mm$, $\xi_0 = 0.5mm$ and $\eta_0 = 0.2mm$

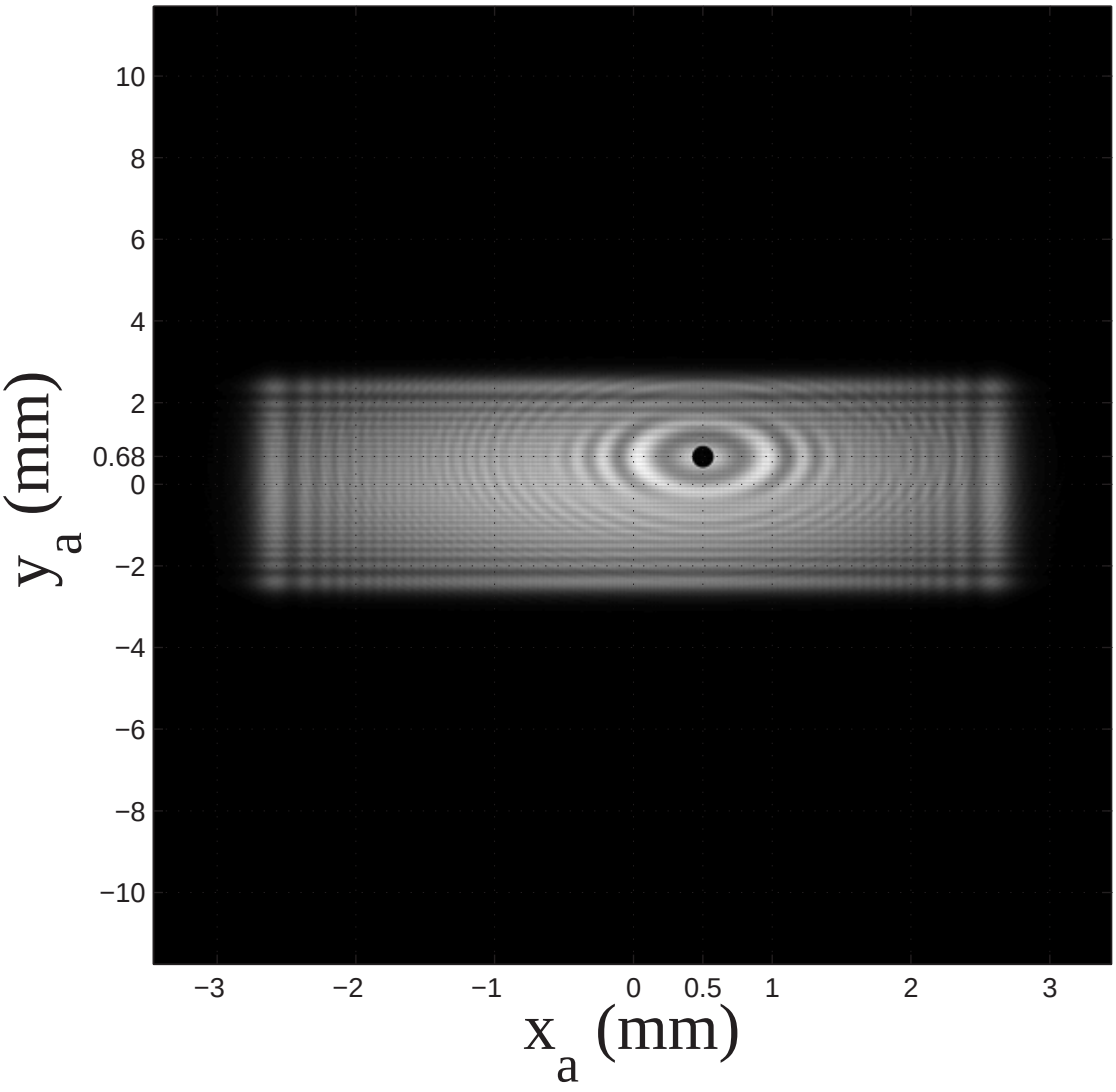

Fig. 4. Fractional Fourier transform of the diffraction pattern with $a_x^{opt} = -0.564$ and $a_y^{opt} = -0.850$

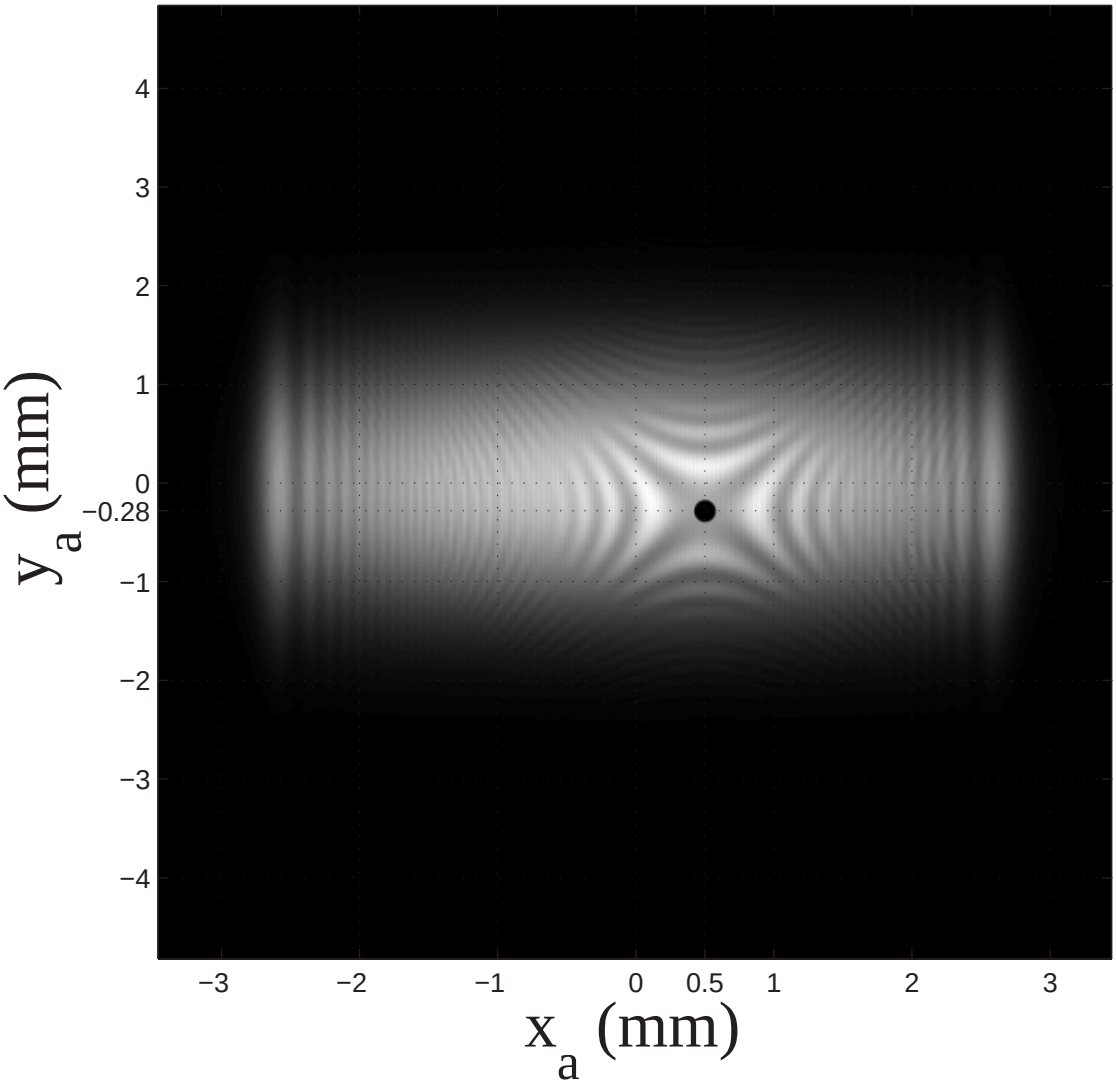

Fig. 5. Fractional Fourier transform of the diffraction pattern with $a_x^{opt} = -0.564$ and $a_y^{opt} = 0.664$

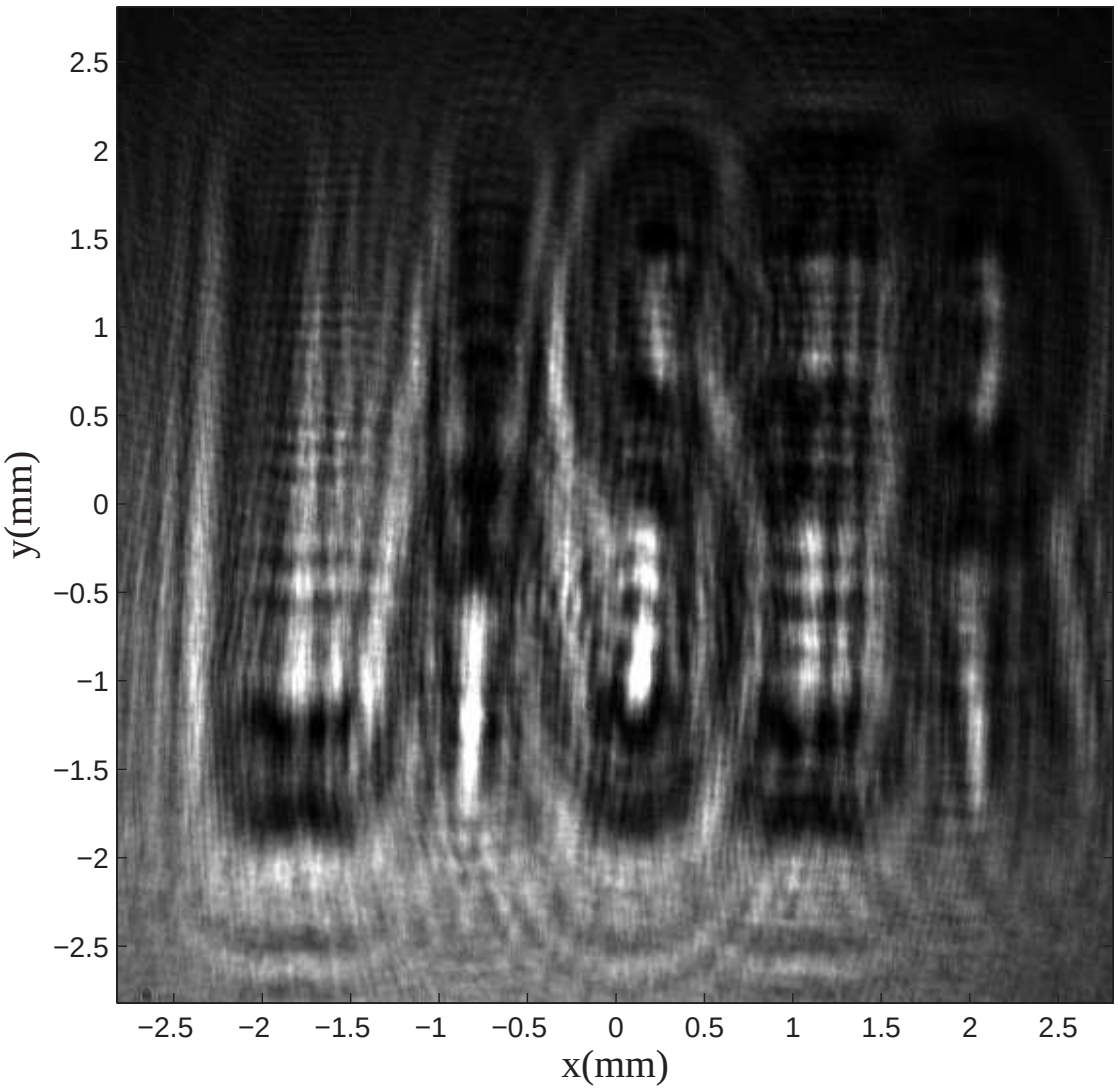

Fig. 6. Diffraction pattern of the world "LASER"

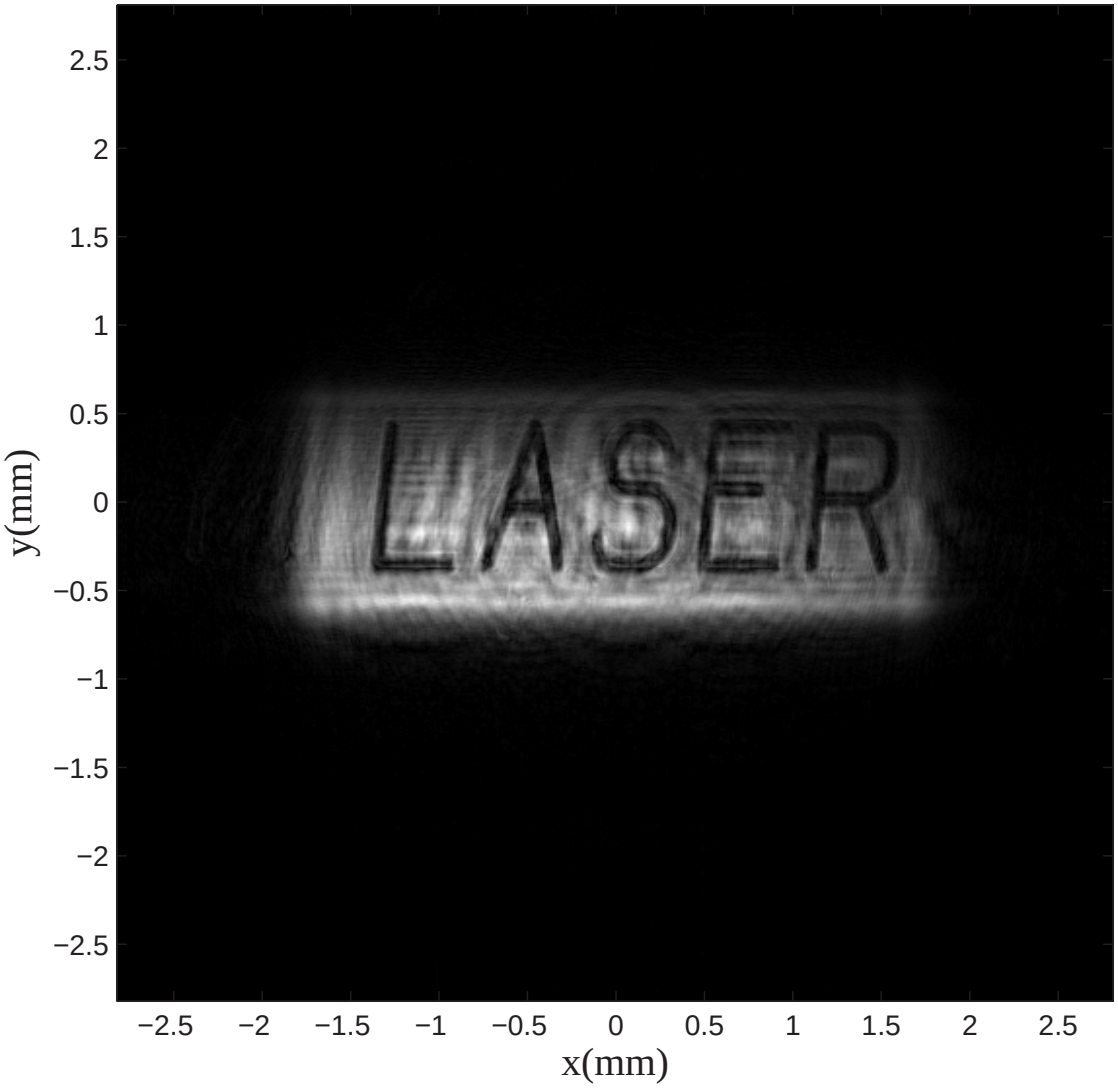

Fig. 7. Fractional Fourier transform of the diffraction pattern with $a_x^{opt} = 0.559$ and $a_y^{opt} = 0.848$